Probe Shapes for Streamwise Momentum and Cross-Stream Turbulence Intensity

Vernon J. Rossow*
NASA Ames Research Center, Moffett Field, California 94035

When the highly turbulent flowfields at the edges of jets, in augmentors, and in other jet-mixing devices are surveyed with conventional pitot probes, the values indicated by the instruments may contain a significant increment brought about by the dynamics of the eddies. Although the influence of turbulence on the measurements is usually negligible in streams where the turbulence level is 1% or less, the effect of turbulence on static and total pressure measurements can be around 20% when the turbulence level exceeds 40%. This paper describes a theoretical study that develops probe shapes that directly measure the time-averaged total pressure based on the streamwise component of the velocity vector to obtain a direct measurement of the streamwise momentum. The difference between the time-averaged pressure indicated by such a probe and one that measures the total head based on the entire velocity vector yields the cross-stream turbulence intensity.

Nomenclature

H = stagnation pressure or total head
p = instantaneous value of static pressure
q = dynamic pressure, $\rho U_\infty^2/2$
R = r/r_p
r = radius
r_e = radius of outer edge of probe face
r_p = probe radius
t = time
$\bar{U}$ = time-averaged velocity in stream direction
u = fluctuating part of velocity component in stream direction
V = instantaneous value of local velocity
v = fluctuating part of velocity component in lateral direction
w = fluctuating part of velocity component in vertical direction
x = distance in streamwise direction
y = distance in lateral direction
z = distance in vertical direction
α = angle of pitch
β = yaw angle
θ = meridian angle
ρ = air density

Subscripts

c = centerline
d = centerline indentation of probe face
e = based on entire instantaneous local velocity
m = measured quantity
orif = orifice
xf = flow across centerline of probe
x = based on x component of velocity
∞ = freestream value

Received July 9, 1990; revision received Oct. 16, 1990; accepted for publication Oct. 16, 1990.

*Senior Scientist, Fixed Wing Aerodynamics Branch. Associate Fellow AIAA.

Introduction

TUBULAR probes have been used for a long time to measure the total and static pressures in a stream to determine its dynamic pressure, velocity, or momentum. Since most of the flowfields where these probes are used have low levels of turbulence (i.e., less than 1%), the measurement of total and static pressures is not influenced, to a measureable extent, by the dynamic pressures associated with the eddies. However, when measurements are desired in flowfields where the turbulence levels are high, the eddies carry with them significant variations in static and dynamic pressures, and they also generate angles of incidence relative to the probe axis large enough to cause significant errors in the measured quantities. Turbulence levels of such a magnitude occur when the flowfield contains energetic shear layers like those found in regions of combustion, along the sides of jets, and in thrust augmentors wherein streams of two different energy levels are mixed and then decelerated. The deceleration lowers the average velocity of the stream without a comparable change in the magnitude and intensity of the eddies. In these kinds of flowfields, the local value of the relative turbulence intensity can exceed 40%. When such a condition is present, the large variations in local flow direction, static pressure, and total head associated with the eddies require that specially designed probe shapes and associated data reduction methods be used to determine the true time-averaged values.

Before going into the development of the probe configurations that will make the desired measurements in highly turbulent streams, the literature was surveyed to find out what sorts of devices were already available. The applicable references[1-38] that were found are listed chronologically to show the advance with time of ideas and probe configurations that have been used to measure total pressure in streams. The use of pressure probes immersed in a stream appears to have started with Pitot in 1732. Pitot's original concept was extended by Prandtl and Tietjens[1] around 1920 to include static pressure by locating orifices in the sidewall of the tube to determine the velocity of the stream through Bernoulli's equation. These probes have been used extensively but do develop significant error in the measurement of both static and total pressure when the inclination of the flow relative to the probe axis is larger than about 10 deg.

A substantial improvement was made in the acceptance angle of total head probes when Kiel[2] introduced the concept of placing a shroud or shield around the nose of the probe. The shroud increases the capability of the probe to recover the entire stagnation pressure to angles of incidence of 45 deg or

more. A number of studies[3-13] were then undertaken to find more versatile designs and to evaluate the various design parameters to minimize measurement errors. Some of the configurations studied are illustrated in Fig. 1. The curves in Fig. 2 (reproduced from Gettleman and Krause[11]) present data on how the stagnation pressure as measured by a variety of these probes is affected by angle of incidence. Also shown for comparison is a cosine-squared curve to be discussed later.

Extension of steady-state concepts to measurements in unsteady or turbulent flowfields was first quantified by Goldstein.[4] His analysis predicts that the effect of turbulence on both the total and static pressures enters the measurement as some factor times the square of the turbulence intensity. Measurements were then made by Fage[5] in ducts of both circular and rectangular cross section that tended to confirm Goldstein's predictions.

Included in the list of references is a group of summary articles[14-35] that describe the guidelines to be followed for probe designs to prevent the need for correction factors in a steady laminar stream. Other techniques which can be used to interpret measurements made in a turbulent stream are, of course, the hot-wire method, laser velocimeter, light-scatter technique,[21] etc.

The relationship between the shape of a probe and its response in a turbulent stream was studied thoroughly by Becker and Brown.[25,26] They first obtained an empirical fit to the response of various total-head probe designs to a steady-state flow angle α. Two constants, K and m, are used to adapt the equation to various experimentally determined response curves similar to those shown in Fig. 2,

$$H_m - H = \tfrac{1}{2}\rho\bar{U}^2[1 - K\,(\sin^2\alpha)^m] \qquad (1)$$

where H_m is the measured stagnation pressure. The authors then incorporate the analytical characteristics of the probes into the statistical properties of turbulence to develop in a sophisticated manner a relationship between the stagnation pressure and the magnitude of the cross-stream turbulence components. They point out that the basis for their quantitative treatment was established by Hinze[17] and that the basic idea in their approach is that, when the turbulence scale is large compared with the critical probe dimensions, the flow around the probe is locally quasisteady, quasi-uniform, and quasilaminar. Under these circumstances, the instantaneous pressure in the probe head is virtually the same as in a steady uniform laminar stream. The difference between the time-averaged pressures measured by a total head probe with a hemispherical nose and a total-head probe with a conical indentation (shown as internal taper in Figs. 1 and 2) is then used to find the mean-square level of the transverse velocity fluctuations. These results were found to be in good agreement with hot-wire measurements, thereby demonstrating that their two-probe method provides a reliable means for determining total head and cross-stream turbulence.

It is noted here that had a probe been available that responds to flow incidence as the cosine squared[17] of the angle, the total head based on the streamwise component of the velocity could have been measured directly. An analysis to interpret the data and find the cross-stream turbulence components would not then have been necessary. Therefore, the objective of the present study is to improve upon the two-probe concept studied by Becker and Brown by developing such a probe or probe-shape criterion. The streamwise total head and the cross-stream turbulence will then be directly available from the measurements without recourse to analysis. Once again, one of the two probes should be a shrouded probe (or one with an internal taper) that has a wide inflow acceptance angle. The second probe, used to measure the total head that results from the streamwise component of the velocity, will have a special nose shape to be described in the text to follow. In brief, the shape of the second total-head probe is such that it has a steady-state response to flow incidence exactly as the cosine squared of the angle; see Fig. 2. A determination of the streamwise momentum also requires a knowledge of the static pressure that can be obtained with a probe or probe system like those described in a companion paper.[39] The present study is limited to subsonic flow wherein the effects of compressibility are negligible. All of the probe shapes considered here are axially symmetric.

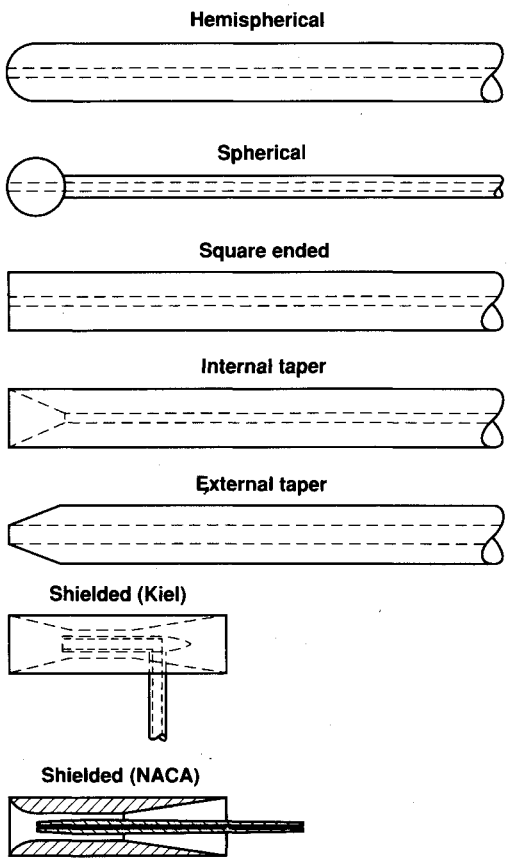

Fig. 1 Typical probe shapes used to measure pitot or stagnation pressure at subsonic speeds; flow direction is from left to right.

Relationships Between Probe Shape, Velocity, and Pressure

The idealized performance of several probes will first be discussed to outline the concepts needed for determining the time-averaged stagnation pressure and the stagnation pressure based on the time-averaged streamwise component of the velocity. In the present discussion it is assumed that the time-av-

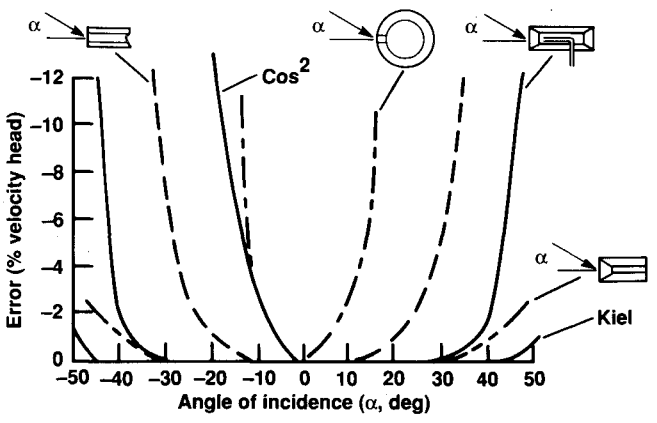

Fig. 2 Response of various total pressure probes to angle of incidence (Gettleman and Krause[11]).

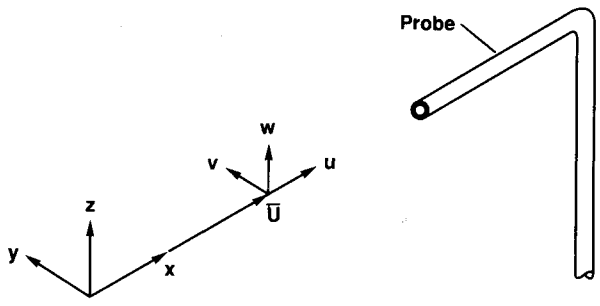

Fig. 3 Diagram of turbulent velocity field and probe.

eraged direction of the stream is aligned with the x axis (see Fig. 3) and that its time-averaged magnitude is given by

$$\bar{U} = \frac{1}{\Delta t}\int_0^{\Delta t} V\,dt \tag{2}$$

The quantity Δt is assumed to be a time interval sufficiently long that the magnitude of the averaged quantity does not change if Δt is increased. The fluctuations of the velocity about this value due to turbulence in the stream are given the instantaneous values u, v, and w that are taken to be aligned with the x, y, and z axes, respectively; see Fig. 3. If the velocity fluctuations vanish, a wide variety of probes recover the sum of the static pressure p and the dynamic pressure $(\rho/2)\bar{U}^2$ for the total head H as given by Bernoulli's equation for incompressible flow, $H = p + (\rho/2)\bar{U}^2$.

To keep track of the various parts of the stream characteristics, a notation is used to define and relate the various pressure magnitudes. The instantaneous total or entire stagnation pressure H_e is based on the local instantaneous static pressure p and the entire instantaneous local velocity V as given by

$$H_e = p + \frac{\rho}{2}V^2 = p + \frac{\rho}{2}[(\bar{U}+u)^2 + v^2 + w^2] \tag{3}$$

and its time-averaged value by

$$\bar{H}_e = \bar{p} + \frac{\rho}{2}(\bar{U}^2 + \bar{u}^2 + \bar{v}^2 + \bar{w}^2) \tag{4}$$

If a probe is used that has a very large acceptance angle (like the Kiel probe or an internally tapered tube, see Figs. 1 and 2), the instantaneous stagnation pressure is given by Eq. (3) and the time-averaged value by Eq. (4). However, the total head used to determine the streamwise momentum is based on the x component of the stream velocity. Its instantaneous value is given by

$$H_x = p + \frac{\rho}{2}(\bar{U}+u)^2 \tag{5}$$

and the time-averaged value by

$$\bar{H}_x = \bar{p} + \frac{\rho}{2\Delta t}\int_0^{\Delta t}(\bar{U}+u)^2\,dt = \bar{p} + \frac{\rho}{2}(\bar{U}^2 + \bar{u}^2) \tag{6}$$

The difference between the two pressures expressed by Eqs. (4) and (6) eliminates both the static pressure and the x component of velocity to yield

$$(\bar{H}_e - \bar{H}_x) = \frac{\rho}{2}(\bar{v}^2 + \bar{w}^2) \tag{7}$$

The design of a probe that measures $\bar{H}_x$ is based on the observation that the instantaneous value of the velocity in the x direction may be written as

$$\bar{U} + u = V\cos\alpha \tag{8}$$

where α is the instantaneous angle of incidence of the local flow relative to the probe axis. The quantity given by Eq. (5) may then be written as

$$H_x = p + \frac{\rho}{2}(V\cos\alpha)^2 \tag{9}$$

In other words, a dynamic pressure based on $V^2\cos^2\alpha$ yields the desired response needed to evaluate the x component of momentum. It then follows that the difference between the entire and the x component of the instantaneous value of the two total heads may be written as

$$H_e - H_x = \frac{\rho}{2}V^2\sin^2\alpha = \frac{\rho}{2}(v^2 + w^2) \tag{10}$$

The foregoing results are usually made dimensionless through division by the dynamic pressure. When the stream has a low turbulence level, the dynamic pressure is easily determined as the difference between the total head and the static pressure. However, when the turbulence level is high, uncertainties in both of these pressures require that the components be evaluated separately and the dimensionless parameters then calculated.

The forms of dynamic pressure available for use include one that is based on the average of the freestream velocity $\bar{U}$,

$$\bar{q} = \frac{\rho}{2}\bar{U}^2 \tag{11}$$

one that is based on the average of the dynamic pressure based on the x component of the streamwise velocity $(\bar{U}+u)$,

$$\bar{q}_x = \frac{\rho}{2}[\bar{U}^2 + \bar{u}^2]$$

and one that is based on the average of the local velocity $\bar{V}$,

$$\bar{q}_e = \frac{\rho}{2}[\bar{U}^2 + \bar{u}^2 + \bar{v}^2 + \bar{w}^2]$$

Under moderate turbulence levels, the three values of dynamic pressure probably will not differ greatly. Since the conventional method used to make velocity components dimensionless is to divide by the time average of the freestream velocity, the dynamic pressure given by Eq. (11) is again used as the reference quantity. Equation (7) may then be written as

$$\frac{(\bar{H}_e - \bar{H}_x)}{\bar{q}} = \frac{(\bar{v}^2 + \bar{w}^2)}{\bar{U}^2} \tag{12}$$

which makes the difference between the two total head measurements directly equal to the sum of the squares of the two cross-stream turbulence levels.

Since the dynamic pressure based on the time-averaged velocity is not directly measured, its magnitude may be estimated by assuming that the three components of turbulence are equal in magnitude so that

$$\frac{\bar{u}^2}{\bar{U}^2} = \frac{(\bar{v}^2 + \bar{w}^2)}{2\bar{U}^2} = \frac{(\bar{H}_e - \bar{H}_x)}{2\bar{q}}$$

The dynamic pressure $\bar{q}$ is then found from $\bar{H}_x$ and the time-averaged static pressure.

Estimate of Inviscid Time-Dependent Effect

It has been pointed out by Corrsin[6] and others that the interaction of a tube with the velocity fluctuations in the stream can be approximated by oscillating the probe in a uniform stream. A theoretical approximation to such an experiment is used here to estimate the effect of velocity fluctua-

tions on the time-averaged pressure sensed by a stagnation pressure probe. The result presented on page 77 of Lamb[40] for the unsteady motion of a body is assumed to apply to the probes under consideration here. The time-dependent effects on pressure arise from the instantaneous velocity field and from the time rate of change of the velocity potential as given by the equation

$$p = \rho \frac{\partial \phi}{\partial t} - \frac{\rho}{2} V^2 + F(t) \tag{13}$$

where $F(t)$ is set equal to zero because the pressure far from the oscillating body is constant with time. The quantity not considered in Eqs. (3-12) for pressure is the expression $(\partial\phi/\partial t)$ in Eq. (13). When the flow is incompressible, the velocity potential is proportional to the instantaneous velocity of the body relative to the fluid. It thereby represents the effect of the time rate of change of the velocity fluctuations on the measured pressures. Since the expression $\rho(\partial\phi/\partial t)$ contains velocity only as the first power, the contribution to the pressure vanishes when an average over time is taken.

The foregoing result, obtained for inviscid flow, probably also applies to viscous flows because the flow over the front of impact-type probes is not greatly influenced by viscous effects or by any flow separation that might occur over the aft parts of the probe. Therefore, a time-dependent effect on pressure does not contribute to the measured time-averaged pressures.

Iterative Design of Probe Shape by Panel Method

Reduction of Problem to a Tractable Analysis

A procedure will now be described for finding probe shapes that have the property that the total head they indicate falls off as the cosine squared of the angle of incidence. As pointed out previously, a measurement made at an orifice on the forward centerline of such a probe would then yield directly the x component of the total head (e.g., Hinze[17]). If the search for shapes that have the cosine-squared characteristic were to be carried out by a trial and error process in a wind tunnel, it would be very tedious and expensive. The more expeditious method is to calculate the inviscid flow over the probe by use of a panel method and then test likely designs in a wind tunnel. The panel code used here was developed at NASA Ames Research Center and is referred to as PMARC.[41,42] The design method is made more expeditious by utilizing the fact that the velocity of approach to the probe when at yaw or angle of incidence consists of one velocity component along the axis of the probe and another perpendicular to the probe axis. Since the velocity fields of the two components are independent of one another, the velocity potentials can be superimposed for a solution that applies when the probe is at yaw; see Fig. 4. Since the two potential flow solutions are independent, the crossflow can be treated separately from the axial flow to find the response function to incidence, defined here as including both angle of attack and of yaw. Since the axial flow component always yields a stagnation point at the orifice that is located at the forward centerline of the probe, it does not contribute to the velocity at the orifice in the determination of the shape. The flow component perpendicular to the probe axis, however, produces a nonzero velocity contribution at the orifice that depends on the shape of the nose of the probe. It remains now to find out what that contribution must be in order to find nose shapes that yield the desired variation.

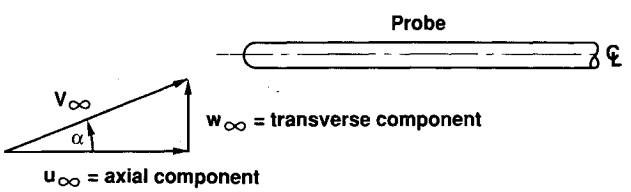

Fig. 4 Resolution of flowfield about probe into axial and transverse components.

The foregoing simplification is carried out by first resolving the freestream velocity about the probe into components along and perpendicular to the probe axis as in Fig. 4:

$$u_\infty = V_\infty \cos\alpha \tag{14a}$$

$$w_\infty = V_\infty \sin\alpha \tag{14b}$$

where the subscript ∞ indicates a point far from the probe. The velocity at the orifice (located on the centerline at the forward face of the probe) as caused by the crossflow component of the freestream velocity is designated by the symbol $W_{xf} = w_{xf}/w_\infty$, where w_∞ is the cross-stream velocity far from the probe. The pressure coefficient at the orifice is then given by

$$C_{p_{xf}} = 1 - W_{xf}^2 \sin^2\alpha \tag{15}$$

As an example of how Eq. (15) works, consider a probe composed of a spherical head mounted on a tube of much smaller diameter. The velocity at an orifice on the forward centerline due to a crossflow is (from potential flow past a sphere) 1.5 times the oncoming flow velocity. From Eq. (15), the pressure coefficient at the orifice as a function of angle of attack is given by

$$C_{p_{xf}} = 1 - (1.5)^2 \sin^2\alpha = 1 - 2.25 \sin^2\alpha$$

and therefore deviates appreciably from a cosine-squared relationship. The comparable expression for a circular cylinder placed along the y axis is given by

$$C_{p_{xf}} = 1 - 4 \sin^2\alpha$$

which also deviates from the desired function.

The problem now is to find a probe shape that has a crossflow velocity of $W_{xf} = 1$ so that the pressure coefficient at the orifice as a function of angle of incidence becomes

$$C_{p_{xf}} = 1 - \sin^2\alpha = \cos^2\alpha \tag{16}$$

which is the variation being sought for the probe that is to measure the total head based on the x component of velocity.

By means of the foregoing step, the problem has been reduced to one wherein the shape of the probes can be found by an iterative process. The analysis proceeds by calculating the flowfield due to a transverse velocity or crossflow over several families of shapes to find out how the parameter W_{xf} is affected by probe shape. By successive iterations, one or more shapes are found wherein $W_{xf} = 1$. The shapes that satisfy such a criterion are then examined to find out which are most easily constructed and which are least sensitive to construction inaccuracies.

General Variation of Centerline Pressure with Nose Shape

To observe how the nose centerline pressures vary with probe shape, the first family of shapes studied consisted of nose shapes that were deviations from a semicircle as given by the equation

$$Z^2 = [X^n - nX]/(1 - n) \tag{17}$$

where the equation is written for the $Y = 0$ plane and the probe is axially symmetric with $X = x/r_p$, $Z = z/r_p$, and n is a parameter that governs the nose profile; see Fig. 5. When $n = 2$, the equation produces a hemispherical nose. When low values of n just above zero are used, shapes are generated that are nearly flat-faced cylinders. Values of n above two produce nose shapes that are rounded but more elongated than hemispherical. The velocity at the orifice location W_{xf} is also presented in Fig. 5 for a range of n values to illustrate how the shape affects the crossflow velocity at the forward centerline

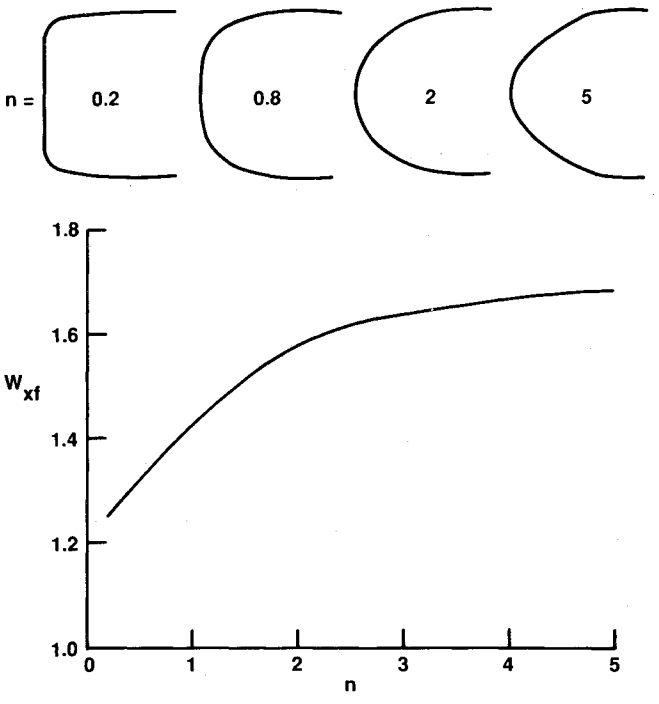

Fig. 5 Across-axis velocity resulting from a transverse stream for nose shapes defined by $Z^2 = [X^n - nX]/(1-n)$.

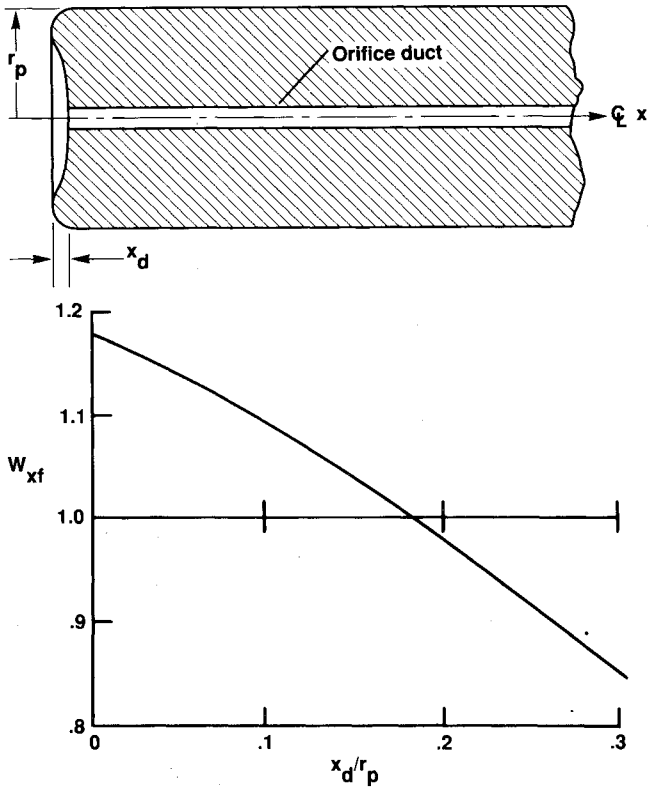

Fig. 6 Typical nose shape with indentation defined by $X = CZ^2(1-Z^2)\,\ell n(\cos\pi Z/2)$ and variation of the across-axis velocity with indentation; cosine-squared variation in measured stagnation pressure is achieved when $W_{xf} = 1.0$.

point for such a family of shapes. As the nose becomes elongated ($n > 2$), the velocity at the orifice W_{xf} approaches an asymptote around 1.7. As the nose becomes more flattened (e.g., $n = 0.2$), the velocity at the orifice decreases but never becomes one or less than one. These results do show, however, that the trend is downward at low values of n, suggesting

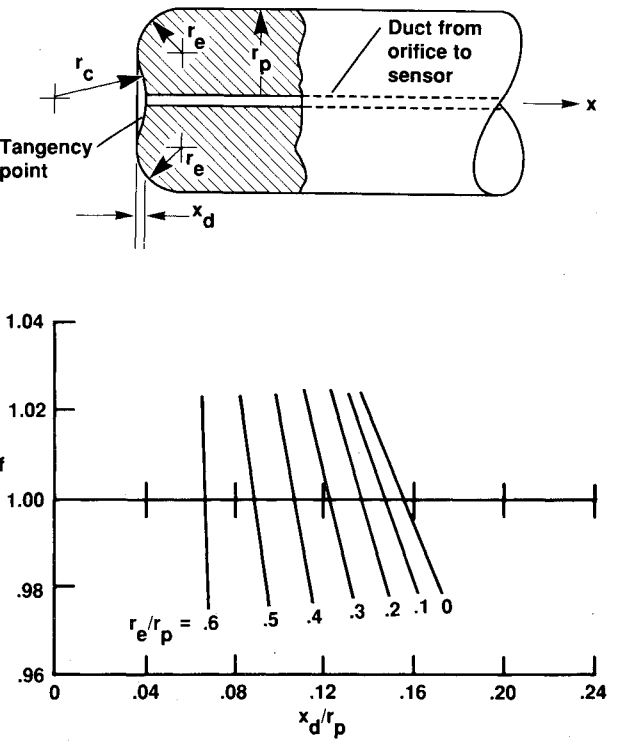

Fig. 7 Typical nose shape defined by circular arcs and the variation of the across-axis velocity as a function of indentation for several edge-radius values; see Eqs. (19–22).

that another family of curves is needed to produce nose shapes that have slightly indented shapes to bring the velocity to one or below.

First Nose Shape with Indentation

To explore how a centerline indentation in the nose shape affects the variation of stagnation pressure with angle of incidence, a family of shapes described by the equation

$$X = CZ^2(1 - Z^2)\,\ell n(\cos\pi Z/2) \tag{18}$$

was then studied; see Fig. 6. The parameter C is a constant that governs the amount of indentation. It was found that an indentation of $X_d = x_d/r_p = 0.18293$ ($C = 0.62717$) yields a value of $W_{xf} = 1$ as desired. The nose shape that corresponds to that condition is shown in Fig. 6 along with a graph of the variation of the centerline velocity W_{xf} for a range of X_d. Although the shapes defined by Eq. (18) would probably function close to the desired way, a disadvantage of these shapes is that the radius at the outer edge of the probe was rather small and very little control was available for the profiles.

Nose Shape Composed of Circular Arcs

The results presented in Figs. 5 and 6 suggest the study of probe shapes composed of circular arcs. Figure 7 presents a typical nose shape and the variation of the centerline velocity with indentation for various edge radii. Equations are presented for the shape as a function of the amount of indentation and of the radius of curvature of the outer edge of the probe. The radius of the circle that defines the shape of the center of the probe is then given by (once again the profile is defined in the $Y = 0$ plane)

$$R_c = [(R_p - R_e)^2 - 2R_eX_d + X_d^2]/2X_d \tag{19}$$

where r_p is the radius of the probe which is used to make the various quantities dimensionless, $R_e = r_e/r_p$ is the radius of the edge, and $X_d = x_d/r_p$ is the amount of indentation at the centerline. The point of tangency of the inner segment of

circular arc and the circular arc that defines the edge radius is given by

$$X_t = X_d[R_e/(R_e + R_c)]$$

$$Z_t = R_c[(R_p - R_e)/(R_e + R_c)]$$

For values of Z less than Z_t, the circle defined by R_c is used to calculate the shape of the probe face by

$$X = X_d - R_c - (R_c^2 - Z^2)^{1/2} \tag{20}$$

and for values of Z greater than Z_t, the edge circle is used to calculate the shape of the probe face by

$$X = R_e - [R_e^2 - (Z - R_p + R_e)^2]^{1/2} \tag{21}$$

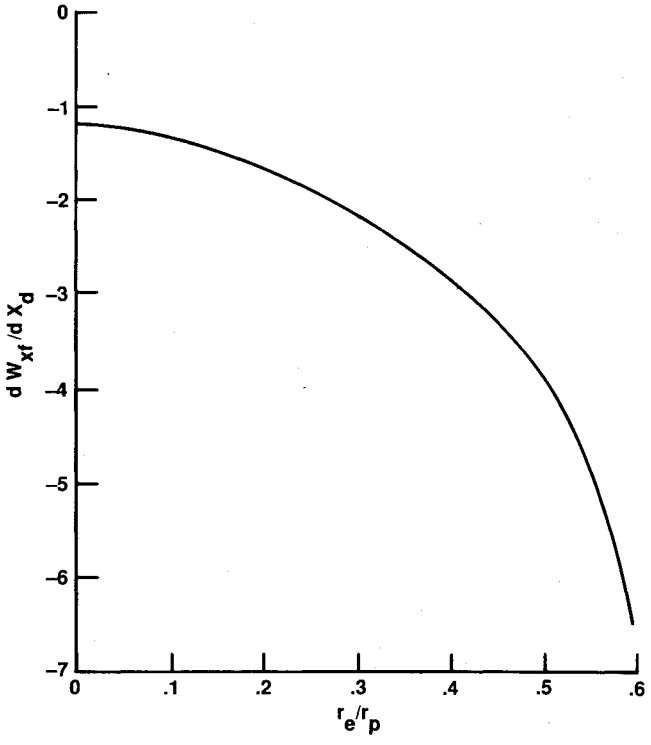

Fig. 8 Variation of sensitivity of centerline velocity to indentation as a function of edge radius when profile is defined by circular arcs; $W_{xf} = 1$.

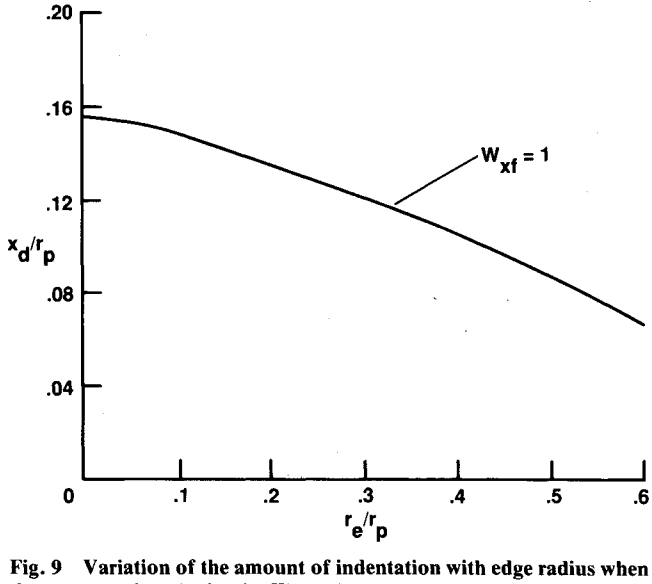

Fig. 9 Variation of the amount of indentation with edge radius when the across-axis velocity is $W_{xf} = 1$ so that the probe will have a cosine-squared response to angle of incidence.

Computations were made on a series of probe shapes made up of circular arcs by use of PMARC[41,42] to determine the velocity at the orifice location on the forward centerline of the probes. A typical nose profile and the results for a series of edge radii are presented in Fig. 7. Successive computer runs used values of x_d/r_p interpolated from these results to find indentations that made the transverse velocity at the orifice equal to w_∞ to four decimal places (i.e., $W_{xf} = 1.0000$). Shape parameters required to achieve such a condition are tabulated in Table 1. It is to be noted in Fig. 7 and in Table 1 that as the edge radius is increased (and the indentation frontal area decreases), the crossflow velocity at the orifice becomes more sensitive to the amount of indentation. This sensitivity is exhibited by the parameter dW_{xf}/dX_d listed in Table 1 and presented graphically in Fig. 8 to show how sensitive the various shapes will be to construction errors. As expected, the larger edge radii are more sensitive to the amount of indentation than the smaller edge radii. This situation occurs because the larger edge radii allow less space for the indentation. As a consequence, more curvature in the probe face is present near the orifice location when larger edge radii are used to achieve the indentation needed for the desired $\cos^2\alpha$ relationship. In fact, when the edge radius is equal to or larger than $0.5r_p$, the circles that describe the edge shape of the probes overlap and limit the amount of indentation according to the equation (see Table 1),

$$X_d = R_e - (2R_e - 1)^{1/2} \tag{22}$$

In purely theoretical terms, the velocity vanishes at the intersection of the two edge circles indicating that a value of $w_{xf}/w_\infty = 1.0000$ is available. Since the indentation is of a very small radial extent, the variation with shape becomes so sensitive to construction errors that use of values above $R_e = 0.6$ is impractical.

Table 1 Values of circular-arc parameters that define probe shapes that have cosine-squared response in stagnation pressure to angle of incidence; $W_{xf} = 1.0000$

$\frac{r_e}{r_p}$	$\frac{x_d}{r_p}$	$\frac{dW_{xf}}{dX_d}$	$\frac{r_c}{r_p}$
0.0	0.1556	− 1.18	3.2902
0.05	0.1542	− 1.22	2.9535
0.1	0.1484	− 1.35	2.7033
0.2	0.1362	− 1.82	2.2181
0.3	0.1222	− 2.12	1.7658
0.4	0.1061	− 2.80	1.3494
0.5	0.0877	− 3.85	0.9692
0.6	0.0668	− 6.67	0.6310

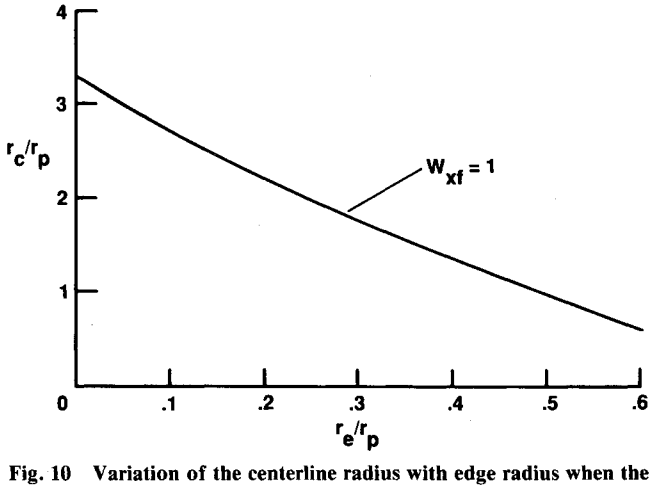

Fig. 10 Variation of the centerline radius with edge radius when the across-axis velocity is $W_{xf} = 1$ so that the probe will have a cosine-squared response to angle of incidence.

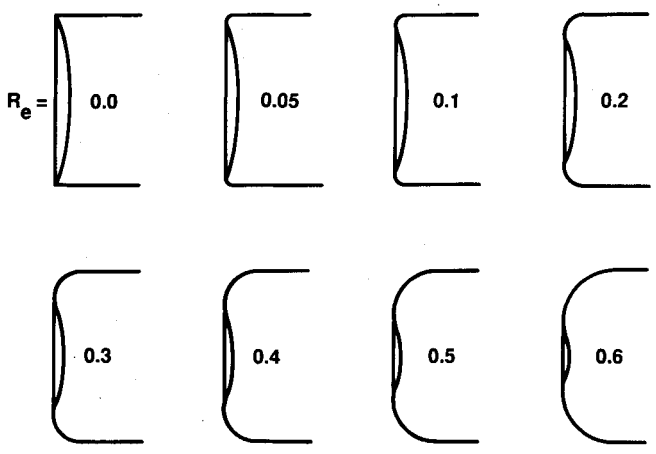

Fig. 11 Nose shapes composed of circular arcs for the cases presented in Table 1.

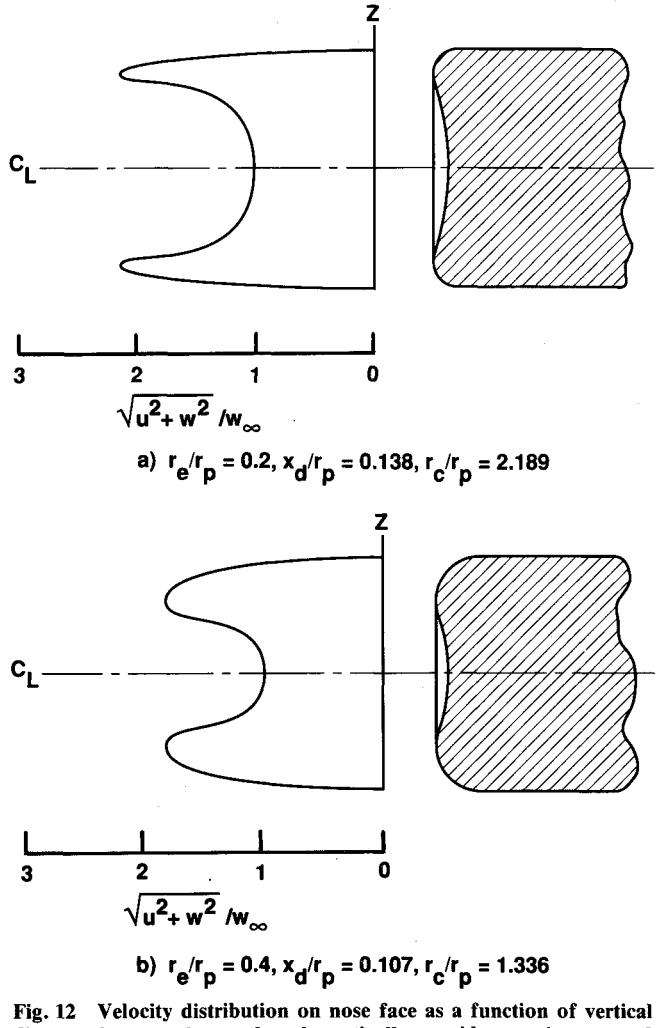

Fig. 12 Velocity distribution on nose face as a function of vertical distance for two shapes that theoretically provide a cosine-squared variation of recovered stagnation pressure with flow incidence.

To complete the presentation of the design parameters, the quantities X_d and R_c are plotted in Figs. 9 and 10 for the condition that $W_{xf} = 1$. The shape of the noses that correspond to the solutions presented in Table 1 are shown in Fig. 11. As expected, the radius of the circle defining the shape of the center of the probe rapidly becomes small at larger values of R_e. These results indicate that a wide range of shapes will produce a probe shape that has a $\cos^2\alpha$ variation in total head with angle of incidence. An optimum or preferred shape does not appear to be indicated. Based on the nature of the flowfield, it seems advisable to choose medium values for the design parameters to achieve a compromise between possible flow separation and construction sensitivity. Such a compromise probably occurs for a value of the edge radius in the range $R_e = r_e/r_p = 0.2$–0.4. The velocity across the face of two such probes is presented in Fig. 12 to illustrate how edge radius changes the region of nearly constant $W_{xf} = 1.0$ that exists near the centerline of the probe. Obviously, the diameter of the orifice used to measure the stagnation pressure should be small enough that it does not extend beyond the radius where the velocity departs appreciably from $W_{xf} = 1.0$.

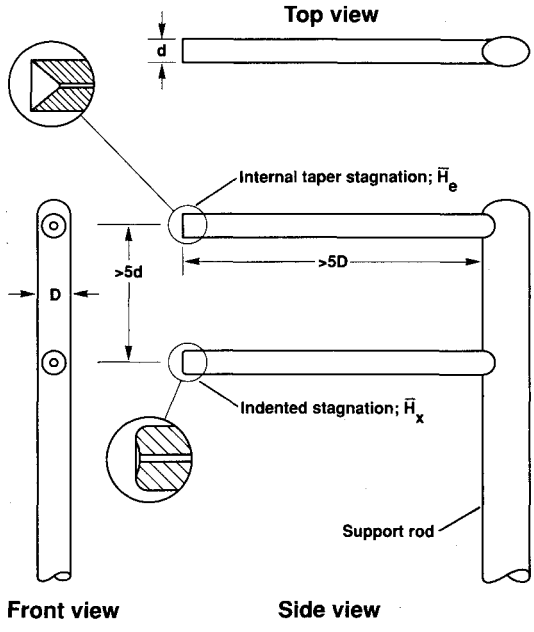

Fig. 13 Diagram of typical two-probe configuration to be used to measure the stagnation pressures based on entire velocity and on the streamwise component of velocity.

To illustrate how a two-probe installation would appear in a test situation, a schematic drawing is presented in Fig. 13. The upper probe is intended to capture the stagnation pressure brought about by the entire velocity vector. Either a shrouded probe[2,8–10] or one with an internal conical taper would accomplish the task. The probe head with an internal taper was chosen because it is easier to construct and occupies less volume. Although Fig. 13 illustrates a conical half angle of around 40 deg, half angles from 15 to 25 deg are to be preferred.[9] As mentioned previously, a wide variety of shapes will probably function satisfactorily for the measurement of the streamwise component of stagnation pressure. The probe head chosen for the illustration is the one composed of circular arcs wherein $r_e/r_p = 0.4$. Both probes are shown on the same support rod so that they would traverse the stream at the same time. As mentioned previously, they could also have been put on separate support rods and surveyed the stream at separate times.

Effect of Manufacturing Errors on Performance

The foregoing analysis specifies the shape of the probe to obtain a cosine-squared variation in total head as a function of flow incidence. The question addressed here is how accurately must the probes be manufactured to achieve engineering accuracy (i.e., three significant figures) in the variation of measured pressure with angle of incidence. Although the velocity at the orifice location is affected by the accuracy of the edge shape, it is probably not necessary to maintain high accuracy on the outer parts of the probe shape. The most sensitive parts of the probe face to construction accuracy is the indentation region. An estimate of the effect of errors in this region is

available through the use of the parameter dW_{xf}/dX_d, as evaluated in the previous section of this paper. From Eq. (15),

$$dC_{p_{xf}}/dX_d = -2W_{xf}(dW_{xf}/dX_d)\sin^2\alpha$$

Hence, the error in pressure coefficient due to an improper value of X_d is directly proportional to the quantity (dW_{xf}/dX_d) which is listed in Table 1 and plotted in Fig. 8.

Another approach is to again consider Eq. (15) and assume that an error in construction has caused W_{xf} to be different from 1.0 by a small amount so that $W_{xf} = 1 + \epsilon$. The quantity ϵ would correspond to the quantity, $(dW_{xf}/dX_d)(\Delta X_d)$, where (ΔX_d) represents a construction inaccuracy. Equation (15) then becomes

$$C_{p_{xf}} = 1 - (1+\epsilon)^2\sin^2\alpha \approx \cos^2\alpha - 2\epsilon\sin^2\alpha$$

where $2\epsilon\sin^2\alpha$ expresses the deviation from the ideal variation to be expected when the surface is not as specified. At small angles of incidence, the errors in pressure are small, but as yaw increases to 20 deg or more, the error in pressure may become measureable.

Concluding Remarks

New probe shapes were introduced to enable the measurement of the streamwise component of total head and the cross-stream turbulence level in highly turbulent streams. It was found that the essential characteristic of the new shape was that the forward face be smoothly contoured with a small amount of indentation. The indentation was found to be necessary to bring about a cosine-squared response to angle of incidence. Although the exact shape of the probe is not unique, a given profile must be determined by analysis or experiment so that the shape yields the desired response. When such a probe has been made, it measures directly the total pressure based on the local static pressure and the x component of the velocity vector. This total head and a measurement of the local static pressure[39] are necessary for the determination of the streamwise momentum. Combination of such a probe with another probe that has a flat response to angle of incidence yields two stagnation pressures that differ by the sum of the squares of the cross-stream turbulence intensities. Probe systems designed in this way provide a simple means for determining the total pressure, streamwise momentum, and turbulence intensity of highly turbulent streams.

References

[1]Prandtl, L., and Tietjens, O. G., *Applied Hydro- and Aeromechanics,* McGraw-Hill, New York, 1934.

[2]Kiel, G., "Total-Head Meter with Small Sensitivity to Yaw," NACA TM 775, Aug. 1935; also *Luftfahrtforschung,* Vol. 12, No. 2, 1935.

[3]Merriam, K. G., and Spaulding, E. R., "Comparative Tests of Pitot-Static Tubes," NACA TN 546, Nov. 1935.

[4]Goldstein, S., "A Note on the Measurement of Total Head and Static Pressure in a Turbulent Stream," *Proceedings of the Royal Society of London,* Series A, Vol. 155, 1936, pp. 570–575.

[5]Fage, A., "On the Static Pressure in Fully-Developed Turbulent Flow," *Proceedings of the Royal Society of London,* Series A, Vol. 155, 1936, pp. 576–596.

[6]Corrsin, S., "Investigation of Flow in an Axially Symmetrical Heated Jet of Air," NACA ARC No. 3L23, Dec. 1943; see also NACA WR W-94.

[7]Huston, W. B., "Accuracy of Airspeed Measurements and Flight Calibration Procedures," NACA TR-919, 1948.

[8]Gracey, W., Letko, W., and Russell, W. R., "Wind-Tunnel Investigation of a Number of Total-Pressure Tubes at High Angles of Attack," NACA TN 2331, April 1951 (supersedes NACA RM L50G19, Sept. 26, 1950).

[9]Gracey, W., Coletti, D. E., and Russell, W. R., "Wind-Tunnel Investigation of a Number of Total-Pressure Tubes at High Angles of Attack—Supersonic Speeds," NACA TN 2261, Jan. 1951.

[10]Russell, W. R., Gracey, W., Letko, W., and Fournier, P. G., "Wind-Tunnel Investigation of Six Shielded Total-Pressure Tubes at High Angles of Attack—Subsonic Speeds," NACA TN 2530, Nov. 1951.

[11]Gettleman, C. C., and Krause, L. N., "Considerations Entering into Selection of Probes for Pressure Measurement in Jet Engines," *Proceedings of the Instrument Society of America,* Vol. 7, 1952, Paper No. 52-12-1, pp. 134–137; see also *Journal of the Instrument Society of America,* Vol. 26, No. 9, 1953, pp. 1385–1388.

[12]Krause, L. N., and Gettleman, C. C., "Effect of Interaction Among Probes, Supports, Duct Walls and Jet Boundaries on Pressure Measurements in Ducts and Jets," *Proceedings of the Instrument Society of America,* Vol. 7, 1952, Paper No. 52-12-2, pp. 138–137; see also *Journal of the Instrument Society of America,* Vol. 26, No. 9, 1953, pp. 1381–1384.

[13]Schulze, W. M., Ashby, G. C., Jr., and Erwin, J. R., "Several Combination Probes for Surveying Static and Total Pressure and Flow Direction," NACA TN 2830, Nov. 1952.

[14]Chambre, P. L., and Schaaf, S. A., "The Impact Tube," *High Speed Aerodynamics and Jet Propulsion,* Physical Measurements in Gas Dynamics and Combustion, Vol. IX, edited by R. W. Ladenburg, Princeton Univ. Press, Princeton, NJ, 1954, pp. 111–135.

[15]Folsom, R. G., "Review of the Pitot Tube," *Transactions of the ASME,* Vol. 78, No. 7, 1956, pp. 1447–1460.

[16]Davies, P. O. A. L., "The Behaviour of a Pitot Tube in Transverse Shear," *Journal of Fluid Mechanics,* Vol. 3, Pt. 5, 1958, pp. 441–456.

[17]Hinze, J. O., *Turbulence—An Introduction to Its Mechanism and Theory,* McGraw-Hill, New York, 1959, pp. 132–139.

[18]Walshe, D. E., and Garner, H. C., "Usefulness of Various Pressure Probes in Fluctuating Low-Speed Flow," British Aeronautical Research Council, Rept. 21,714, F. M. 2917, Feb. 1960.

[19]Salter, C., Warsap, J. H., and Goodman, D. G., "A Discussion of Pitot-Static Tubes and of Their Calibration Factors with a Description of Various Versions of a New Design," British Aeronautical Research Council, R. and M. No. 3365, 1965.

[20]Jezdinsky, V., "Measurement of Turbulence by Pressure Probes," *AIAA Journal,* Vol. 4, No. 11, 1966, pp. 2072,2073.

[21]Becker, H. A., Hottel, H. C., and Williams, G. C., "On the Light-Scatter Technique for the Study of Turbulence and Mixing," *Journal of Fluid Mechanics,* Vol. 30, Pt. 2, 1967, pp. 259–284.

[22]Becker, H. A., Hottel, H. C., and Williams, G. C., "The Nozzle-Fluid Concentration Field of the Round, Turbulent, Free Jet," *Journal of Fluid Mechanics,* Vol. 30, Pt. 2, 1967, pp. 285–304.

[23]Schlichting, H., *Boundary-Layer Theory,* 3rd ed., McGraw-Hill, New York, 1968.

[24]Dudziniski, T. J., and Krause, L. N., "Effect of Inlet Geometry on Flow-Angle Characteristics of Miniature Total-Pressure Tubes," NASA TN D-6406, July 1971.

[25]Becker, H. A., and Brown, A. P. G., "Response Functions for Pitot Probes in Turbulent Streams," Queens Univ., Kingston, Ontario, Canada, Thermal and Fluid Sciences Group Rept. 2-72, May 1972.

[26]Becker, H. A., and Brown, A. P. G., "Response of Pitot Probes in Turbulent Streams," *Journal of Fluid Mechanics,* Vol. 62, Pt. 1, 1974, pp. 85–114.

[27]Chue, S. H., "Pressure Probes for Fluid Measurement," *Progress in Aerospace Sciences,* Vol. 16, No. 2, 1975, pp. 147–223.

[28]Bertelrud, A., "Flow Disturbances Associated with Preston Tubes in Turbulent Boundary Layers," Aeronautical Research Inst. of Sweden, Rept. 127, Stockholm, Jan. 1977.

[29]Raghava, A. K., Kumar, K. L., Malhotra, R. C., and Agrawal, D. P., "A Novel Arrangement for the Measurement of the Velocity Vector," *Journal of Physics E: Scientific Instruments,* Vol. 10, 1977, pp. 844–846.

[30]Holman, J. P., and Gajda, W. J., Jr., *Experimental Methods for Engineers,* 3rd ed., McGraw-Hill, New York, 1978, pp. 253–258.

[31]Mitchell, W. J., Blagun, B. E., Johnson, D. E., and Midgett, M. R., "Angular Flow Insensitive Pitot Tube Suitable for Use with Standard Stack Testing Equipment," U. S. Environmental Monitoring and Support Lab., Rept. EPA 600/4-79-042, Cincinnati, OH, June 1979.

[32]Huffman, G. D., Rabe, D. C., and Poti, N. D., "Flow Direction Probes from a Theoretical and Experimental Point of View," *Journal of Physics E: Scientific Instruments,* Vol. 13, July 1980, pp. 751–760.

[33]Christiansen, T., and Bradshaw, P., "Effect of Turbulence on Pressure Probes," *Journal of Physics E: Scientific Instruments,* Vol. 14, 1981, pp. 992–997.

[34]Goldstein, R. J., *Fluid Mechanics Measurements,* Hemisphere, Washington, DC, 1983.

[35]Ostowari, C., and Wentz, W. H., Jr., "Modified Calibration

Technique of a Five-Hole Probe for High Flow Angles," *Experiments in Fluids,* Vol. 1, 1983, pp. 166-168.

[36]Samet, M., and Einav, S., "Directional Pressure Probe," *Reviews of Scientific Instruments,* Vol. 55, No. 4, 1984, pp. 582-588.

[37]Chu, J. K., Rios-Chiquete, E., Sarohia, S., and Bernstein, L., "The 'Chu-Tube': A Velocimeter for Use in Highly-Sheared, Three-Dimensional Steady Flows," *Aeronautical Quarterly,* Vol. 91, No. 903, 1987, pp. 142-149.

[38]Jenkins, R. C., "Effects of Pitot Probe Shape on Measurement of Flow Turbulence," *AIAA Journal,* Vol. 25, No. 6, 1987, pp. 889-892.

[39]Rossow, V. J., "Probe Systems for Static Pressure and Cross-Stream Turbulence Intensity," *Journal of Aircraft,* Vol. 28, No. 11, 1991, pp. 750-755.

[40]Lamb, H., Hydrodynamics, 6th ed., Dover, New York, 1932.

[41]Ashby, D. L., Dudley, M. R., and Iguchi, S. K., "Development and Validation of an Advanced Low-Order Panel Method," NASA TM-101024, Oct. 1988.

[42]Ashby, D. L., Dudley, M. R., Iguchi, S. K., Browne, L., and Katz, J., "Potential Flow Theory and Operation Guide for the Panel Code PMARC," NASA TM-102851, Aug. 1990.